Dalton Transactions

Accepted Manuscript

This article can be cited before page numbers have been issued, to do this please use: A. Hazari, L. K. Das, R. M. Kadam, A. Bauza, A. Frontera and A. Ghosh, *Dalton Trans.*, 2015, DOI: 10.1039/C4DT03446E.

ROYAL SOCIETY OF CHEMISTRY

www.rsc.org/dalton

View Article Online
DOI: 10.1039/C4DT03446E

Graphical Abstract

Unprecedented structural variations in trinuclear mixed valence Co(II/III) complexes derived from a Schiff base and its reduced form: Theoretical studies, pnicogen bonding interactions and catecholase-like activities

Alokesh Hazari, Lakshmi Kanta Das, Ramakant M. Kadam, Antonio Bauzá, Antonio Frontera* and Ashutosh Ghosh*

Solvent induced *cis* and *trans* forms of a mixed valence trinuclear Co(II/III) complex with a salen type Schiff base ligand are isolated. The reduction of the Schiff base results in the formation of an unprecedented cyclic trinuclear mixed valence Co(II/III) complex in which a $\mu_{1,3}$-N_3 coordinated azido ligand participates in pnicogen bonding interactions established by DFT calculations. The catecholase like activities in the aerial oxidation of 3,5-di-tert-butylcatechol to the corresponding o-quinone of all three complexes have been examined.

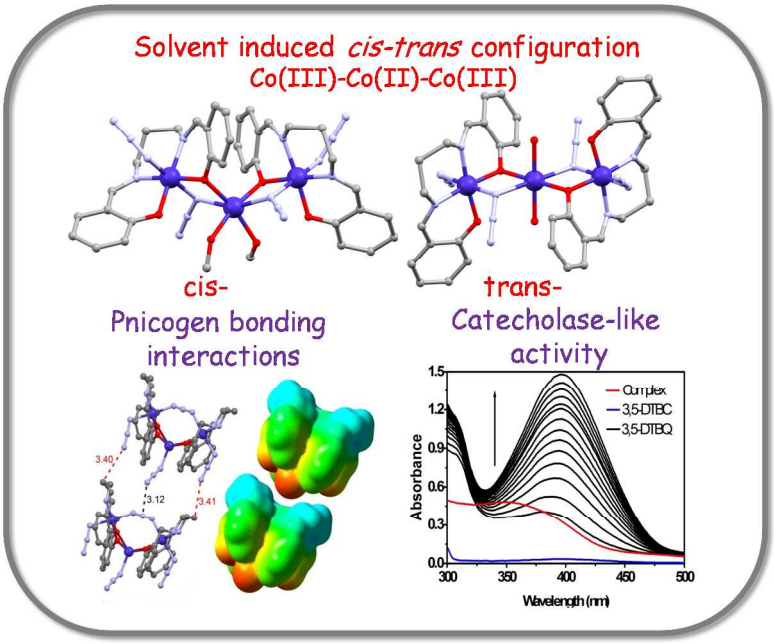

View Article Online
DOI: 10.1039/C4DT03446E

Cite this: DOI: 10.1039/c0xx00000x

www.rsc.org/xxxxxx

ARTICLE TYPE

Unprecedented structural variations in trinuclear mixed valence Co(II/III) complexes derived from a Schiff base and its reduced form: Theoretical studies, pnicogen bonding interactions and catecholase-like activities

Alokesh Hazari,[a] Lakshmi Kanta Das,[a] Ramakant M. Kadam,[b] Antonio Bauzá,[c] Antonio Frontera*[c] and Ashutosh Ghosh*[a]

Received (in XXX, XXX) XthXXXXXXXXX 20XX, Accepted Xth XXXXXXXXX 20XX
DOI: 10.1039/b000000x

Three new mixed valence trinuclear Co(II/III) compounds *cis*-$[Co_3L_2(MeOH)_2(N_3)_2(\mu_{1,1}\text{-}N_3)_2]$ (**1**), *trans*-$[Co_3L_2(H_2O)_2(N_3)_2(\mu_{1,1}\text{-}N_3)_2]\cdot(H_2O)_2$ (**2**) and $[Co_3L^R{}_2(N_3)_3(\mu_{1,3}\text{-}N_3)]$ (**3**) have been synthesized by reacting a di-Schiff base ligand (H_2L) or its reduced form $[H_2L^R]$ (where H_2L = N,N′-bis(salicylidene)-1,3-propanediamine and H_2L^R = N,N′-bis(2- hydroxybenzyl)-1,3-propanediamine) with cobalt perchlorate hexahydrate and sodium azide. All three products have been characterized by IR, UV-Vis and EPR spectroscopies, ESI-MS, elemental, powder and single crystal X-ray diffraction analyses. Complex **1** is an angular trinuclear species in which two terminal octahedral $Co(III)N_2O_4$ centers coordinate to the central octahedral cobalt(II) ion through μ_2-phenoxido oxygen and $\mu_{1,1}$-azido nitrogen atoms along with two mutually *cis*-oxygen atoms of methanol molecules. On the other hand, in linear trinuclear complex **2**, in addition to the μ_2-phenoxido and $\mu_{1,1}$-azido bridges with terminal octahedral Co(III) centres, the central Co(II) is bonded with two mutually *trans*-oxygen atoms of water molecules. Thus the *cis*-*trans* configuration of the central Co(II) is solvent dependent. In complex **3**, the two terminal octahedral $Co(III)N_2O_4$ centers coordinate to the central penta-coordinated Co(II) ion through double phenoxido bridges along with nitrogen atom of a terminal azido ligand. In addition, the two terminal Co(III) are connected through a $\mu_{1,3}$-azido bridge that participates in pnicogen bonding interactions (intermoluclar N–N interaction) as acceptors. Both the *cis* and *trans* isomeric forms of **1** and **2** have been optimized using density functional theory (DFT) calculations and it is found that the *cis* configuration is energetically more favorable than the *trans* one. However, *trans* configuration of **2** is stabilized by the hydrogen bonding network involving a water dimer. The pnicogen bonding interactions have been demonstrated using MEP surfaces and CSD search which support the counter intuitive electron acceptor ability of the $\mu_{1,3}$-azido ligand. Complexes **1**–**3** exhibit catecholase-like activities in the aerial oxidation of 3,5-di-tert-butylcatechol to the corresponding *o*-quinone. Kinetic data analyses of this oxidation reaction in acetonitrile reveal that the catecholase-like activity follows the order: **1** (k_{cat} = 142 h^{-1}) >**3**(k_{cat} = 99 h^{-1}) >**2** (k_{cat} = 85 h^{-1}). Mechanistic investigations of the catalytic behaviors by X-band EPR spectroscopy and estimation of hydrogen peroxide formation indicate that the oxidation reaction proceeds through the reduction of Co(III) to Co(II).

Introduction

Cobalt complexes derived from Schiff bases have attracted an extensive interest in the area of coordination chemistry due to their intriguing structural features and various applications covering catalysis in organic synthesis, photochemistry, electrochemistry and important biological applications.[1–4] The salen-type di-Schiff base ligands on reaction with Co(II) in an aerobic condition are known to afford mixed valence tri-nuclear complexes.[5] The main structural feature of these complexes is a central Co(II) ion linked to two terminal Co(III) ions through double phenoxido bridges along with an additional anionic bridge between the terminal and central cobalt atoms, which is usually a carboxylate group[6] except three examples where this bridge is chloride, azido, or sulphito.[7–9] It is interesting to mention that in most of such complexes the two anionic bridges are mutually *cis* excepting one in which two mutually *trans*-acetate ions link the terminal Co(III) to central Co(II).[10] This feature is somewhat extraordinary as the similar homo- and hetero-trinuclear complexes of divalent metal ions (Mn(II), Co(II), Ni(II),Cu(II), Zn(II)) are abundant with various anionic coligands (e.g. carboxylate, azide, cyanate, etc) and usually these bridges are mutually *trans* to each other.[11–15]

Recently, it has been shown that the use of reduced Schiff base ligands may bring about fascinating variations in the structure of the complexes mainly due to fact that (i) the reduction of the rigid azomethine (–CH=N–) fragment to less constrained $–CH_2–NH–$ moiety make them more flexible compared to the Schiff bases[16] and (ii) the introduction of a H-atom on the nitrogen not only has considerable effect on the crystal packing but it can even stabilize rather unusual isomers.[17]

In this present investigation, our aim is to synthesize mixed valence cobalt complexes using a salen-type di-Schiff base ligand and its corresponding reduced analogue along with azide as coligand in order to study their structural variations and catecholase-like activities.[18] Catecholase-like activity of some model coordination complexes has been a topic of recent interest for the development of new bioinspired catalysts.[19] Catechol oxidase is a copper-containing type-III active-site protein that catalyzes the oxidation reaction of a wide range of *o*-diphenols (catechols) to corresponding *o*-quinones through a process known as catecholase activity. From the reports of distinguished research groups, the ability of dicopper complexes to oxidize phenols and catechols is well established.[20] From these extensive studies, it is concluded that various structural factors such as metal−metal distances, electrochemical properties of the complexes,

View Article Online
DOI: 10.1039/C4DT03446E

exogenous bridging ligands, the ligand structure, and the pH can influence the catecholase activity.[19–21] Furthermore, the mechanistic studies for the oxidation of catecholic substrate to their respective quinone reveals that the reaction proceeds through the formation of either a dicopper(II) catecholate intermediate or an organic radical intermediate such as copper(I) semiquinonate.[22] Recent investigations have also shown that some manganese(II/III), nickel(II), zinc(II) and cobalt(II/III) species can also mediate such catechol oxidation.[23–26] It becomes evident that in the case of Ni(II) and Mn(III) metal-centered redox participation is most probably responsible for the catecholase activity of these model compounds whereas in case of redox innocent Zn(II) this activity can be promoted through the generation of ligand-centered radical. However, to the best of our knowledge, no mechanistic studies have yet been done on the catecholase-like activity of cobalt complexes.

In this report, we have synthesized and structurally characterized two mixed valence trinucler complexes *cis*-$[Co_3L_2(MeOH)_2(N_3)_2(\mu_{1,1}\text{-}N_3)_2]$ (**1**) and *trans*-$[Co_3L_2(H_2O)_2(N_3)_2(\mu_{1,1}\text{-}N_3)_2]\cdot(H_2O)_2$ (**2**) by reacting a di-Schiff base ligand (H_2L) (where H_2L = N,N′-bis(salicylidene)-1,3-propanediamine), cobalt perchlorate hexahydrate and sodium azide in two different solvents, methanol and ethanol, respectively. Two solvent molecules (methanol or water) which coordinate to the central Co(II) are *cis* in **1** but *trans* in **2**. Another complex, $[Co_3L^R{}_2(N_3)_3(\mu_{1,3}\text{-}N_3)]$ (**3**) has been synthesized with the reduced form of this Schiff base ligand, N,N′-bis(2-hydroxybenzyl)-1,3-propanediamine (H_2L^R). The unique feature of **3** is a $\mu_{1,3}$-N_3 bridge between two terminal Co(III) and its participation in pnicogen bonding interactions as acceptor. Theoretical study has been performed using DFT calculations at the BP86-D3/def2-TZVP level of theory, to analyze (i) the energy difference between the *cis-trans* isomers, (ii) how the solvent molecule influences the stability of the isomers, (iii) the probable explanation for the isolation of both the isomers in the solid state, and (iv) some non-covalent interactions including pnicogen bonding interactions[27] observed in the crystal packing of complex **3**. To the best of our knowledge, the *cis-trans* configurational changes in mixed valentCo(III)–Co(II)–Co(III) as in **1** and **2,** and the presence of pnicogen interaction in azide in **3** are unprecedented. All three complexes show catecholase-like activity. The EPR spectral investigation reveals that the process is most likely associated with the reduction of cobalt(III) to cobalt(II), as proposed for the copper-based models of this biocatalyst.

Experimental

Starting Materials

The salicylaldehyde, 1,3-propanediamine and sodium borohydride were purchased from Lancaster and were of reagent grade. They were used without further purification.

Caution! Azide salts and Perchlorate salts of metal complexes with organic ligands are potentially explosive. Only a small amount of material should be prepared and it should be handled with care.

Synthesis of the Schiff Base Ligand, N,N′-bis(salicylidene)-1,3-propanediamine (H_2L)

The Schiff base ligand was synthesized by a reported method.[28] 5 mmol of 1,3-propanediamine (0.42 mL) was mixed with 10 mmol of the salicylaldehyde (1.04 mL) in methanol or ethanol (20 mL). The resulting solution was refluxed for *ca.* 2 h and allowed to cool. The resulting yellow solution of the ligand was purified by removing methanol completely from the resultant solution under vacuum to result in a viscous liquid, followed by addition of a mixture of petroleum ether and chloroform. The extracted pure yellow solid mass of ligand was dissolved in methanol or ethanol and used for complexation. The ligand was characterized by elemental analyses and ^{1}H NMR study.

Ligand (H_2L). Anal. Calcd for $C_{17}H_{18}N_2O_2$: C 72.32, H 6.43, N 9.92; Found: C 72.48, H 6.69, N 10.05%. ^{1}H-NMR ($CDCl_3$, 300 MHz) (Fig. S1) in ppm: h = 2.08-2.17 (m, 2H, CH_2); g = 3.746-3.704 (t, 2H, CH_2); b,c,d and e = 6.863-7.348 (aromatic H); a = 8.380 (S, 1H,CH=N-)

Synthesis of the reduced Schiff base ligand, N,N'-bis(2-hydroxybenzyl)-1,3-propanediamine (H_2L^R)

The di-Schiff base ligand (H_2L) was synthesized as stated above. Then 20 mL (5 mmol) of this prepared methanolic ligand solution (H_2L) was cooled to 0°C, and solid sodium borohydride (570 mg, 15 mmol) was added to this methanolic solution with stirring. After completion of addition, the resulting solution was acidified with concentrated HCl (10 mL) and then evaporated to dryness.[29] The reduced Schiff base ligand H_2L^R was extracted from the solid mass with methanol. The ligand was purified in same procedure as described above for H_2L. The purified ligand was dissolved in methanol and used for complexation.

Ligand (H_2L^R). Anal. Calcd for $C_{17}H_{22}N_2O_2$: C 71.30, H 7.74, N 9.78; Found: C 71.48, H 7.69, N 9.65%. ^{1}H-NMR ($CDCl_3$, 300 MHz) (Fig. S2) in ppm: h = 1.68-1.82 (m, 2H, -CH_2); k = 2.08 (s, H, -NH) g = 2.71-3.79 (m, 2H, -CH_2); a = 3.99 (s, 2H, -CH_2) b,c,d and e = 6.75-7.19 (aromatic H).

Synthesis of the complex *cis*-$[Co_3L_2(MeOH)_2(N_3)_2(\mu_{1,1}\text{-}N_3)_2]$ (1)

The yellow colored methanolic solution (20 mL) of the di-Schiff base (H_2L) ligand (2 mmol) was taken in a beaker. To this methanolic solution, a water solution (1 mL) of $Co(ClO_4)_2\cdot 6H_2O$ (1.098 g, 3 mmol) followed by an aqueous solution (1 mL) of sodium azide (0.260 g, 4mmol) was added. The mixture was stirred for 1 h and then filtered. The filtrate was allowed to stand overnight when needle shaped dark brown X-ray quality single crystals of **1** appeared at the bottom of the beaker. The crystals were washed with a methanol−water mixture and dried in a desiccator containing anhydrous $CaCl_2$ and then characterized by elemental analysis, spectroscopic methods, and X-ray diffraction.

Complex **1**: Yield: 0.834 g, 86%. Anal. Calc. for $C_{36}H_{40}Co_3N_{16}O_6$: C 44.59, H 4.16, N 23.11; found: C 44.72, H 4.35, N 22.95%; UV/vis: [λ_{max} in nm (ε_{max} in M^{-1} cm^{-1})] (MeCN) = 618(379), 377(21661), and 276(17532) and λ_{max} in nm (solid, reflectance) = 617 and 378. IR (KBr) in cm^{-1}: ν(C=N) 1621, ν(N_3) 2061 and 2010. HRMS (m/z, ESI$^+$): found for $[CoL(Na)]^+$ = 362.0504 (calc. 362.0441), $[Co_2L_2(CH_3CN)Na]^+$ = 743.1162 (calc. 743.1284), $[Co_3L_2(N_3)_3]^+$ = 863.0811 (calc. 863.0696).

Synthesis of the complex, *trans*-$[Co_3L_2(H_2O)_2(N_3)_2(\mu_{1,1}\text{-}N_3)_2]\cdot(H_2O)_2$ (2)

Complex **2** was prepared by mixing the same components in the same stoichiometric ratio as for **1** but using ethanol instead of methanol as solvent. In this case, square shaped blackish brown X-ray quality single crystals appeared at the bottom of the vessel on keeping the filtrate at open atmosphere.

Complex **2**: Yield: 0.694 g, 71%. Anal. Calc. for $C_{34}H_{40}Co_3N_{16}O_8$: C 41.77, H 4.12, N 22.92; found: C 41.54, H 4.32, N 23.06%; UV/vis: [λ_{max} in nm (ε_{max} in M^{-1} cm^{-1})] (MeCN) = 619(512), 398(26274), and 272(17537) and λ_{max}in nm (solid, reflectance) = 620 and 399. IR (KBr) in cm^{-1}: ν(C=N) 1621, ν(N_3) 2062 and 2010, HRMS (m/z, ESI+): found for $[CoL(Na)]^+$ = 362.0431 (calc. 362.0441), $[Co_2L_2\ (CH_3CN)\ Na]^+$ = 743.1058 (calc. 742.1284), $[Co_3L_2(N_3)_3]^+$ = 863.0678 (calc. 863.0696).

View Article Online
DOI: 10.1039/C4DT03446E

Synthesis of the complex $[Co_3L^R(N_3)_3(\mu_{1,3}\text{-}N_3)]$ (3)

Complex **3** was prepared using reduced Schiff base ligand with the same molar ratios of reactant as for **1** and **2**. To the colourless methanolic solution (20 mL) of the reduced Schiff base ligand (H_2L^R), a water solution (1 mL) of $Co(ClO_4)_2{\cdot}6H_2O$ (1.098 g, 3 mmol) followed by an aqueous solution (1 mL) of sodium azide (0.260 g, 4 mmol) were added. The mixture was stirred for 1 h and then filtered. The filtrate was allowed to stand overnight when rhombic shaped deep brown X-ray quality single crystals of complex **3** appeared at the bottom of the beaker.

Complex **3**: Yield: 0.840 g, 92%. Anal. Calc. for $C_{34}H_{40}Co_3N_{16}O_4$: C 44.70, H 4.41, N 24.53; found: C 44.83, H 4.31, N 24.65%; UV/vis: [λ_{max} in nm (ε_{max} in M^{-1} cm^{-1})] (MeCN) = 624(167), 363(16010), and 254(16492) and λ_{max} in nm (solid, reflectance) = 621 and 365. IR (KBr) in cm^{-1}: ν(N-H) 3235, ν(N_3) 2051 and 2027, HRMS (m/z, ESI^+): found for $[CoL^R(Na)]^+$ = 366.0747 (calc. 366.0754) and $[Co_3L^R{}_2(N_3)_4Na]^+$ = 936.1290 (calc. 936.1312).

Physical Measurements

Elemental analyses (C, H, and N) were performed using a Perkin-Elmer 2400 series II CHN analyzer. IR spectra in KBr pellets (4000−400 cm^{-1}) were recorded using a Perkin- Elmer RXI FT-IR spectrophotometer. Electronic spectra in acetonitrile (800−200 nm) and solid state (800−300 nm) were recorded in a Hitachi U-3501 spectrophotometer. The ^{1}H-NMR spectra at 300 MHz were recorded in $CDCl_3$ on a Bruker DRX 300 spectrometer. The electrospray ionization mass spectrometry (ESI-MS positive) spectra were recorded with a Micromass Qtof YA 105 mass spectrometer. EPR spectra was recorded on a Bruker EMM 1843 spectrometer operating at X-band frequency (9.80 GHz), having 100 kHz frequency modulation and a phase sensitive detection to obtain a first derivative signal. Di phenyl picrylhydrazyl (DPPH) was used for calibration of g-values of paramagnetic species. The epr parameters for different samples have been precisely determined from the calculated spectra, as obtained from Bruker SIMFONIA program based on perturbation theory R.T. Weber, (WIN-EPR SIMFONIA manual, 1995).[30]

Crystallographic data collection and refinement

Well formed single crystal of each complex was mounted on a Bruker-AXS SMART APEX II diffractometer equipped with a graphite monochromator and Mo Kα (λ = 0.71073 Å) radiation. The crystals were positioned 60 mm from the CCD, and frames (360) were measured with a counting time of 5 s. The structures were solved using the Patterson method through the SHELXS 97 program. Non hydrogen atoms were refined with independent anisotropic displacement parameters, while difference Fourier synthesis and least-squares refinement showed the positions of any remaining non-hydrogen atoms. The non-hydrogen atoms were refined with anisotropic thermal parameters. The hydrogen atoms bound to carbon atoms were included in geometric positions and given thermal parameters equivalent to 1.2 (or 1.5 for methyl groups) times those of the atom to which they were attached. Hydrogen atoms that bonded to N or O were located in a difference Fourier map and refined with distance constraints. Successful convergence was indicated by the maximum shift/error of 0.001 for the last cycle of the least-squares refinement. Owing to the intrinsic nature of the crystal **1**, the reflection data were weak and thus R factors are high. Absorption corrections were carried out using the SADABS program,[31] while all calculations were made via SHELXS 97,[32] SHELXL 97,[33] PLATON 99,[34] ORTEP-32,[35] and WINGX system ver-1.64.[36] Data collection, structure refinement parameters, and crystallographic data for the three complexes are given in Table S1.

Theoretical methods

The energies of all complexes included in this study were computed at the BP86-D3/def2-TZVP level of theory. The geometries have been fully optimized for the energetic analysis of the *cis/trans* isomerism. Instead, we have used the crystallographic coordinates for the theoretical analysis of the non-covalent interactions observed in the solid state. The calculations have been performed by using the program TURBOMOLE version 6.5.[37] For the calculations we have used the BP86 functional with the latest available correction for dispersion (D3).[38] The Bader's "Atoms in molecules" theory has been used to study the interactions discussed herein by means of the AIM all calculation package.[39]

This level of theory has been shown useful and reliable to study noncovalent interactions like those analyzed herein.[28,40] Moreover, the optimized complexes 1 and 2 exhibit Co–N and Co–O metal ligand distances that are similar to the experimental ones. For instance, in complex **1** the experimental distances range from 1.90 to 2.12 Å and the theoretical ones range from 1.98 to 2.21 Å.

Catalytic Oxidation of 3,5-DTBC

The catecholase activity of **1**−**3**, were studied using 3,5-di-tert-butylcatechol (3,5-DTBC) as substrate in acetonitrile solution under aerobic conditions at room temperature. The reactions were followed spectrophotometrically by monitoring the increase in the maximum absorbance of the quinone band at 400 nm as a function of time (time scan). To detect the formation of hydrogen peroxide during the catalytic reaction we followed the iodometric method as reported earlier.[40]

Results and Discussion

Syntheses of the Complexes

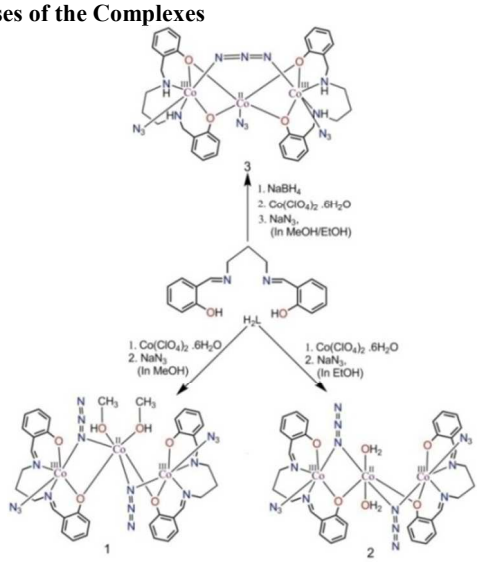

Scheme 1 Formation of the complexes **1**–**3**.

The Schiff-base ligand (H_2L) and its reduced analouge (H_2L^R) were synthesized using the reported procedures.[28,29] The Schiff-base ligand (H_2L) on reaction with cobalt perchlorate hexahydrate and sodium azide in 2:3:4 molar ratios resulted two different trinuclear mixed valence Co(II/III) complexes, *cis*-$[Co_3L_2(MeOH)_2(N_3)_2(\mu_{1,1}\text{-}N_3)_2]$ (**1**) and *trans*-$[Co_3L_2(H_2O)_2(N_3)_2(\mu_{1,1}\text{-}N_3)_2]{\cdot}(H_2O)_2$ (**2**) depending upon the solvent used. Complex **1** separated as a needle shaped dark brown single crystals from methanolic filtrate whereas complex **2**

View Article Online
DOI: 10.1039/C4DT03446E

separated as square shaped blackish brown single crystals from ethanolic filtrate. On the other hand, when the reduced Schiff-base ligand, cobalt perchlorate hexahydrate and sodium azide were mixed in same molar ratio as for **1** and **2** in MeOH then rhombic shaped deep brown X-ray quality single crystals of **3** was isolated from the reaction mixture (Scheme 1). It may also be noted that no complex other than complex **3** was produced when the same reaction was carried out in ethanol medium.

IR and UV−Vis Spectra of the complexes

Besides elemental analysis, all three complexes were initially characterized by the IR spectra. A strong and sharp band due to the azomethine υ(C=N) group of the Schiff base appears at 1621 cm^{-1} for both of the complexes **1** and **2** (Fig. S3−S4). On the other hand, a moderately strong and sharp peak at 3235 cm^{-1} (due to a N−H stretching vibration) and absence of any peak at around 1620 cm^{-1}, for complex **3** (Fig. S5) indicate that the imine group of the Schiff base is reduced.[41] In addition, the presence of azido ligands in all three complexes is confirmed by the appearance of strong and sharp peaks at 2061, 2062 and 2051 cm^{-1} along with shoulders at 2010, 2010 and 2027 cm^{-1} in the spectra of **1**–**3** respectively (Fig. S3−S5). The splitting of the band is indicative of the presence of two different coordinated azide ions[42] in agreement with their crystal structures.

The electronic spectra of these compounds were recorded in acetonitrile solutions and in solid state. The complexes show a broad absorption band in the visible region at 618, 619, and 624 nm in acetonitrile and 617, 620, and 621 nm in the solid state for **1**–**3** respectively, attributed to d−d transitions of Co(II) ions. Besides these bands, an absorption band in the range 363−399 nm were observed in solution as well as solid state, assignable to ligand-to-metal charge transfer transitions for all three complexes. Moreover, absorption bands at 276, 272 and 254 nm in acetonitrile were observed for **1**–**3** respectively (Fig. S6–S7), assignable to intra-ligand charge transfer transitions.

Description of the structures (1–3)

A partially labeled diagram of complex **1** is presented in Fig. 1, and selected bond parameters are summarized in Table 1. The molecular structure of **1** contains two discrete neutral trinuclear units (**1A** and **1B**) of same formula, *cis*-$[Co_3L_2(MeOH)_2(N_3)_2(\mu_{1,1}\text{-}N_3)_2]$ with slight differences in bond parameters. Thus, we describe only the structure of **1A**. In the structure, three cobalt atoms are in bent arrangement with ∠Co(3A)−Co(1A)−Co(2A) angle of 130.4°. Each of the cobalt atoms has a six-coordinated distorted octahedral geometry. The basal plane of the two terminal Co(III) centers are formed by two μ_2-phenoxido O atoms and two imine N atoms of the chelated dianionic tetradentate Schiff-base ligand $[L^{2-}]$ and the axial positions are occupied by one nitrogen atom of $\mu_{1,1}$-bridging azido and one nitrogen from terminal azido ligand. The basally coordinated atoms and the Co atom deviate only slightly from the mean plane of the coordinated atoms (Table S2). The basal Co–O bond distances in each of the terminal cobalts are shorter than basal Co–N bond distances and the axial Co−N bond distances are longer than the basal bonds (Table 1). Both the bridging and terminal of azido ligands are nearly linear (Table S3). The ranges of *trans* [170.9(5)–176.7(4)°] and *cis* [80.2(4)–96.8(4)°] angles (Table 2) indicate slight deviation from ideal octahedral geometry.

The central Co(II) atom is bonded to two phenoxido oxygen atoms of deprotonated tetradentate Schiff base ligands, two nitrogen atoms of $\mu_{1,1}$-bridging azide ions and two oxygen atoms of methanol molecules. Here also, the Co(II)–N bond distances are slightly greater than Co(II)–O bond distances (Table 1) like the terminal cobalt atoms. The central Co−N/O bond distances are significantly greater than that of the terminal cobalt centers as the central cobalt atom is in +2 oxidation states whereas terminals atoms are in +3 oxidation states. The range of *cis* angles [73.4(4)–92.5(4)°] and *trans* angles [157.6(4)°–168.7(4)°] around Co(II) indicate considerable deviation from the ideal values. The two methanol molecules in this structure are mutually *cis* to each other as usual to other mixed valence cobalt complexes reported previously.[5-9] The Co(3A)···Co(1A) and Co(2A)···Co(1A) distances are 3.169 and 3.169 Å, respectively.

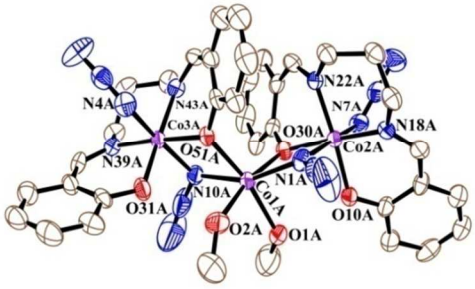

Fig. 1 The structure of **1** with ellipsoids at 50% probability. The structure contains two similar discrete neutral trinuclear units (**1A** and **1B**) of same formula. One unit (**1A**) is shown here. Hydrogen atoms have been omitted for clarity.

The structure of **2** is shown in Fig. 2 together with the atomic numbering scheme. Dimensions in the metal coordination sphere are given in Table 2. The centrosymmetric linear trinuclear unit of this complex having molecular formula $[Co_3L_2(H_2O)_2(N_3)_2(\mu_{1,1}\text{-}N_3)_2]\cdot(H_2O)_2$, contains two mutually *trans* water molecule unlike **1**. Like **1**, the basal plane of the terminal Co(III) centers are formed by two phenoxido oxygen atoms and two imine nitrogen atoms of the chelated dianionic tetradentate Schiff-base ligand $[L^{2-}]$ and the axial positions are occupied by one nitrogen atom of $\mu_{1,1}$-bridging azido and one nitrogen from terminal azido ligand. Here also, the terminal Co atom deviate from the mean plane of the coordinated atoms and this deviation is smaller than that in complex **1** (Table S2). The Co–O bond distances are shorter than Co–N bond distances in the basal plane and the axial Co−N bond distances are longer than the basal bonds (Table 2) like **1**. The bridging and terminal of azido ligands in this structure are also nearly linear (Table S3). The ranges of *trans* [173.0(5)–177.4(6)°] and *cis* [83.9(5)–96.5(6)º] angles (Table 3) indicate similar deviation from ideal octahedral geometry as in **1**.

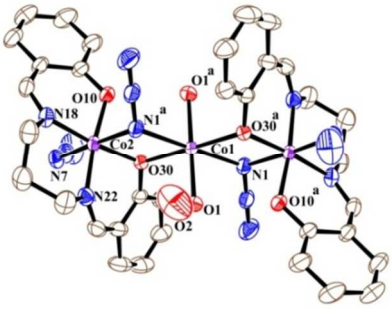

Fig. 2 The structure of **2** with ellipsoids at 50% probability. Symmetry element [a] = 2-x,-y,-z. Hydrogen atoms have been omitted for clarity.

The central cobalt atom Co(1), which sits on the crystallographic inversion center has a six-coordinated distorted octahedral geometry. The basal plane of this atom is constructed by two μ_2-phenoxido oxygen atoms of deprotonated tetradentate Schiff base ligands and two nitrogen atoms of $\mu_{1,1}$-bridging azide ions. Two

View Article Online
DOI: 10.1039/C4DT03446E

*trans*axial positions are occupied by two water molecules. The central Co–N/O bond distances are significantly greater (Table 2) than that of the terminal cobalt center as expected. Though all the trans angles of Co(1) are 180º (as the molecule is centrosymmetric), the range of *cis* angles [87.9(5)–104.3(5)°] deviates considerably from their ideal value (90°). The metal-metal distance (Co(2)···Co(1)) in this case is slightly smaller than that in complex **1** (3.132 Å).

The structure of complex **3** having molecular formula $[Co_3L^R{}_2(N_3)_3(\mu_{1,3}\text{-}N_3)]$ (**3**) is shown in Fig. 3. Selected bond lengths and angles are listed in Table 3. In this structure, three cobalt atoms are in a bent arrangement with ∠Co(3)–Co(1)–Co(2) angle of 104.2º. The terminal cobalt(III) atoms present a six-coordinated distorted octahedral geometry like other two structures described above. The basal plane of the two terminal Co(III) centers are formed by two phenoxido oxygen atoms and two imine nitrogen atoms of the chelated dianionic tetradentate reduce Schiff-base ligand $(L^R)^{2-}$ and the axial positions are occupied by one nitrogen atom of $\mu_{1,3}$-bridging azido and one nitrogen from terminal azido ligand. The terminal Co atoms deviate only slightly from the mean plane of the coordinated atoms and these deviations are the smaller than **1** but greater than **2** (Table S2). The basal Co–O bond distances in each of the terminal cobalt atoms are shorter than basal Co–N bond distances and the axial Co−N bond distances are larger than the basal bonds (Table 3). Both the bridging and terminal of azido ligands are nearly linear (Table S3) like other two structures. The ranges of *cis* [78.5(2)–96.4(3)º for Co(2) and 87.2(2)–96.0(2)º for Co(3)] and the *trans* angles [170.9(2)–175.1(2)º for Co(2) and 171.2(2)–175.1(2)º for Co(3)] indicate slight deviation from ideal octahedral geometry.

Unlike other two structures, here the central cobalt atom is penta-coordinated by four phenoxido oxygen atoms of two reduced Schiff base ligands, and a terminally coordinating azido ligand. The distortions of the coordination geometry from the square pyramid to the trigonal bipyramid have been calculated by the Addison parameter (τ).[43]The value of τ is defined as the difference between the two largest donor metal-donor angles divided by 60. The τ is 0 for the ideal square pyramid and 1 for the trigonal bipyramid. The τ value of Co(1) is 0.46, indicating that the geometry is intermediate between the two ideal geometries. The metal–metal distances (Co(3)···Co(1) 3.122 Å and Co(2)···Co(1) 3.121 Å) are similar to those of **2**.

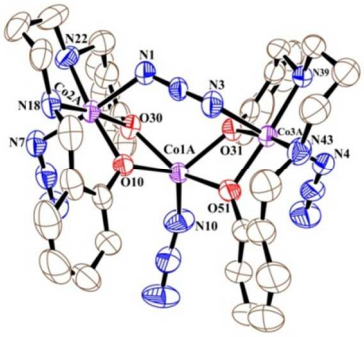

Fig. 3 The structure of **3** with ellipsoids at 50% probability. Hydrogen atoms have been omitted for clarity.

A CSD search for trinuclear Co(III)–Co(II)–Co(III) complexes containing deprotonated tetradentate Schiff base ligand revels that only nine such structures have been reported so far.[5,6-9,10] Among them, eight complexes are linear in which terminal Co(III) and central Co(II) are linked through acetato (six structures)[5,6,10] or sulfite[9] (one structure) or chlorido[7] (one structure) bridges in addition to double phenoxido bridges. The remaining one is azido bridged,[8] angular trinuclear species in which central Co(II) is connected to terminal Co(III) *via* single phenoxido bridges and two mutually *cis*-oxygen atoms of water molecules are bonded with Co(II). Thus this structure is very similar to that of compound **1** of present study. It is to be noted that in eight of these complexes, the two anionic bridges that link the terminal Co(III) to central Co(II) are mutually *cis* and only in one[10] these bridges are mutually *trans*. Therefore, the structure of complex **2** of the present work, in which the two water molecules are trans coordinated to the central Co(II) is rather unusual. Moreover, complexes **1** and **2** present the first example of the formation of "*cis*-*trans*" configuration induced by the solvent molecule for this type of trinuclear complexes. Complex **3** is the first example of mixed valence Co(II/III) complexes with reduced salen type di-Schiff base ligands and possesses a unique structural feature among these mixed-valence complexes. That is, two terminal Co(III) are joined by a $\mu_{1,3}$-azido bridge with a penta-coordinated central Co(II). CSD search shows that there are few reports where $\mu_{1,3}$-azido bridge connects the first metal ions with the third one in the fragments of polynuclear (>3 metal centers) complexes but only one hit is there of a trinuclear complex containing Cu(II) that has such interaction.[44]

Theoretical study

The three trinuclear Co(III)−Co(II)−Co(III) compounds that have been X-ray characterized and are represented in Figs. 1-3. As aforementioned, two different compounds are obtained depending on the solvent used. That is, compound **1** (obtained from methanol) presents the two coordinated methanol molecules in *cis* position of Co(II) whilst compound **2** (obtained from ethanol) exhibits two *trans* coordinated water molecules. Moreover, when the Schiff base ligand is reduced, a totally different structure **3** is obtained.

In order to give an explanation to the aforementioned experimental results we have fully optimized the complex **1** in *cis* conformation starting from the crystallographic coordinates of **1** and in *trans* starting from the crystallographic coordinates of **2** and replacing the coordinated water molecules by methanol moieties. The resulting optimized geometries are shown in Fig. 4 where we also indicate the relative energies. It can be observed that for compound **1** the *cis* conformation is 10.5 kcal/mol more stable than the *trans* in agreement with experiment. Using the same methodology we have optimized the *cis* and *trans* isomers for compound **2** and, similarly to compound **1**, the *cis* isomer is also considerably more favorable than the *trans* isomer (18.0 kcal/mol). Examining the intramolecular interactions, it can be observed that both isomers exhibit two strong (O–H···O) hydrogen bonds involving the hydrogen atoms of the coordinated water molecules and the phenolic oxygen atom. Moreover the *cis* isomers also present aromatic interactions involving the arene rings (highlighted in Fig. 4) and CH_2 groups of the ligands. These interactions further stabilize the *cis* isomer. This result does not agree with the experimental X-ray structure obtained for compound **2** (*trans* isomer). A likely explanation is that intermolecular interactions in the solid state stabilize the *trans* isomer in compound **2**. A further examination of compound **2** reveals the crucial role of the uncoordinated water molecules that form a hydrogen bonding network connecting the coordinated water molecules with the end-on coordinated azide ligands (see Fig. 5). This hydrogen bonding network cannot be formed in the *cis* isomer due to the relative position of the coordinated water molecules and the azide ligands. Moreover, it is not possible in compound **1**, where methanol instead of water is coordinated to the metal center.

View Article Online
DOI: 10.1039/C4DT03446E

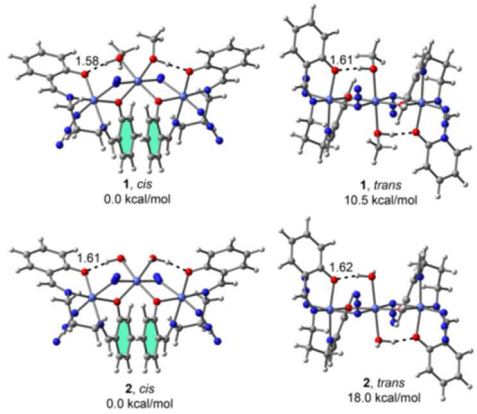

Fig. 4 BP86-D3/def2-TZVP optimized geometries of the cis/trans isomers of compounds **1** and **2**. Relative energies are also indicated. Distances in Å.

We have computed the interaction energy of compound **2** with the water molecules since this should compensate the 18 kcal/mol difference between the *cis* and *trans* isomers of compound **2**. The reaction used to compute this energy (denoted as ΔE_w) is shown in Fig. 5 and it can be observed that ΔE_w clearly compensates the *cis-trans* energetic difference (18.0 kcal/mol) providing a plausible explanation to the different behavior of both compounds in the solid state.

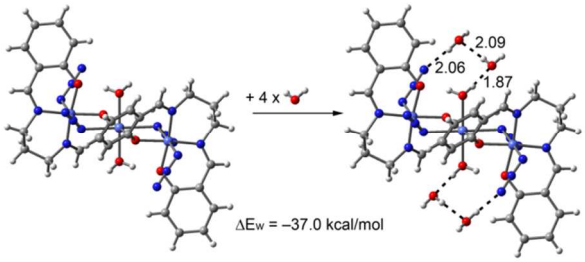

Fig. 5 Hydrogen bonding network observed in the solid state of compound **2** and the associated interaction energy

In the second part of the theoretical study we analyze the dual behavior of the azide ligand since it is able to act as a H-bond acceptor (electron rich moiety) when it is end-on coordinated or acting as a $\mu_{1,1}$ bridging ligand and as electron acceptor (middle nitrogen atom) when it is acting as $\mu_{1,3}$–N_3 bridging ligand. In the description of the experimental structures (*vide* supra) and in Fig. 5 hydrogen bonding interactions involving the azide ligand are described. In Fig. 6 we show Molecular electrostatic potential surface (MEPS) of compound **3** that presents a $\mu_{1,3}$–N_3 bridging ligand in the structure together with several end-on coordinated azido ligands. Interestingly, it exhibits two well defined regions, one with positive potential (blue region) close to the $\mu_{1,3}$–N_3 bridging ligand and the other with negative potential close to the end-on azide ligand. Therefore, azide-azide (pnicogen bonding) interaction can be expected involving two nitrogen atoms, one acting as donor and the other one as acceptor.

In sharp agreement with the MEP surface analysis, a pnicogen bonding[27] interaction is observed in the crystal packing of compound **3** (see Fig. 7). This arrangement maximizes the electrostatic interaction, as can be observed by the high degree of complementarity of the MEP surfaces. Therefore, the $\mu_{1,3}$–N_3 coordination mode of the azido ligand drastically changes their electron donor by electron acceptor ability using the π-hole of the central nitrogen atom. The interaction energy of this dimer is large and negative not only due to pnicogen bonding but also several C–H···N interactions (Table S4) that also contribute to the total binding energy (see red dashed lines in Fig. 7).

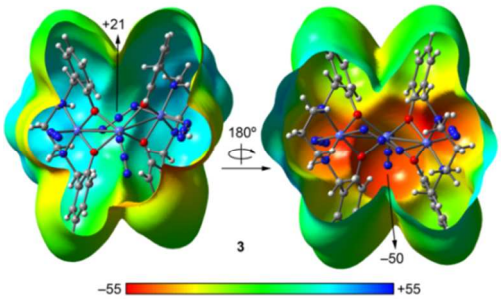

Fig. 6 Molecular Electrostatic Potential surface of compound **3** in two orientations. Energies in kcal/mol.

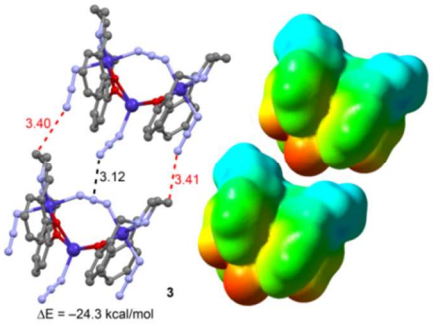

Fig. 7 Left: partial view of the crystal packing of compound **3** with indication of the N···N interaction. The complementary MEP surfaces are also indicated in the same orientation. Hydrogen atoms have been omitted for clarity.

Finally, we have performed a search in the Cambridge Structural Database (CSD) in order to know if pnicogen bonding interactions are common in $\mu_{1,3}$–N_3 coordinated azide ligands. It is well-known that the CSD is a convenient and reliable tool for analyzing geometrical parameters.[45] Interestingly, we have found 20 X-ray structures where the $\mu_{1,3}$–N_3 ligand coordinated to transition metals participates in pnicogen π–hole interactions as acceptor (π stands for the π-system of azide). Some examples are shown in Fig. 8 illustrating the importance of this interaction in the solid state. In some examples the electron donor is a neutral moiety (CAPVOF[46] and MILROP[47]) and in others it is an anion (LIJCUC[48] and MILROP[49]). The lp/anion–π-hole interaction distances range 3.01–3.28 Å, in agreement with previous theoretical and experimental studies on similar interactions involving the nitro/nitrate group.[50] As far as our knowledge extends, the description of such interaction in azide is unprecedented.

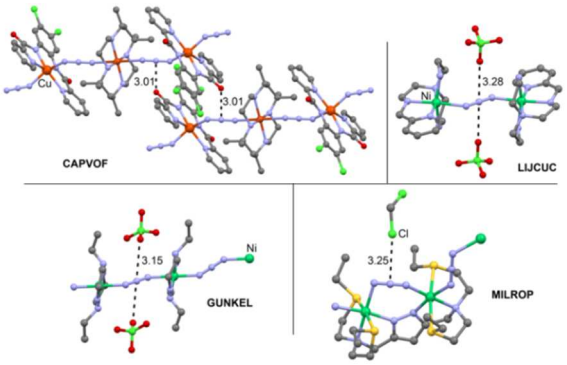

Fig. 8 Partial views of several X-ray structures retrieved from the CSD. Distances in Å. Hydrogen atoms have been omitted for clarity.

View Article Online
DOI: 10.1039/C4DT03446E

Catechol Oxidase Studies and Kinetics.

The catecholase-like activity of three mixed valence Co(II/III) complexes were determined by the catalytic oxidation of 3,5-DTBC. This substrate is most widely used because of its low redox potential which facilitates oxidation to quinone, and its bulky substituents, which prevent further oxidation reactions such as ring opening.[51] Moreover, the oxidation product, 3,5-di-tert-butylquinone (3,5-DTBQ), is highly stable and a characteristic absorption band maxima appeared at around 400 nm (ε = 1900 $M^{-1}cm^{-1}$) in pure acetonitrile solvent system. Before going into the detail of kinetics studies, we examined the catalytic activity of complexes **1**–**3** for oxidation of 3,5-di-tert-butylcatechol (3,5-DTBC) to corresponding *o*-quinone (3,5-DTBQ) in acetonitrile solvent according to the reaction shown in Scheme 2.

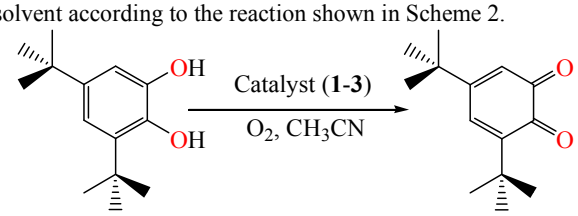

Scheme 2 Catalytic oxidation of 3,5-DTBC to 3,5-DTBQ in acetonitrile solvent.

For this purpose, 10^{-4} (M) acetonitrile solutions of these three complexes were treated with 100 equivalent of 3,5-DTBC at room temperature under aerobic conditions. After mixing of the 3,5-DTBC into the complexes (**1–3**), the progress of the reaction was followed by recording the UV-Vis spectra of the mixtures at 5 min time's interval. The gradual increase of an absorption band at around 400 nm corresponds to 3,5-DTBQ[52] was observed for complexes **1**–**3**. The variation of the spectral behavior of complex **1** in the presence of 3,5-DTBC is shown in Fig. 9. Similar plots for **2** and **3** are contained in the Supporting Information (Fig. S8 and S9).

The kinetics of oxidation of 3,5-DTBC to 3,5-DTBQ by the complexes were determined by the method of initial rates by monitoring the growth of the quinone band at 400 nm as a function of time. The rate constant for a particular complex-substrate mixture was determined from the $\log[A_\alpha/(A_\alpha - A_t)]$ *vs* time plot. The oxidation rates and various kinetic parameters of the substrate concentration were determined by using 10^{-4} M solutions of **1**–**3** with different concentrations of 3,5-DTBC under aerobic conditions. In each cases, a first-order kinetic was observed at low concentrations of 3,5-DTBC, whereas higher concentrations resulted in saturation kinetics. The observed rates *versus* concentration of substrate data were then analyzed on the basis of the Michaelis−Menten approach of enzymatic kinetics to get the Lineweaver−Burk (double reciprocal) plot and values of kinetic parameters V_{max}, K_M, and K_{cat}. Both the curves of observed rate *vs* [substrate] and Lineweaver−Burk plot for complex **1** are shown in Fig. 10. Similar plots for **2** and **3** are given in the Supporting Information (Fig. S10 and S11). The kinetic parameters for all the cases are listed in Table 4. The k_{cat} values can be calculated by dividing the V_{max} values by the concentration of the corresponding complexes (Table 4). The k_{cat}(in h^{-1}) values are 142, 85 and 99 for **1**–**3,** respectively. Thus, the catecholase-like activity follows the order: complex **1**> complex **3**> complex **2**. These values lie in the range of the k_{cat} values of the di-copper(II) systems behaving as functional models of catechol oxidase. Thus, these three mixed valence Co(III)−Co(II) compounds can also be considered as a functional model of catechol oxidase. It is important to mention that, the k_{cat} values obtained for complexes **1**–**3** are significantly higher than those reported for di-cobalt(II) compounds containing "end-off" compartmental Schiff base ligand[53] (Table 5) and considerably lower than those reported for dinuclear mixed-valence Co(III)−Co(II) complexes derived from a macrocyclic ligand.[54]

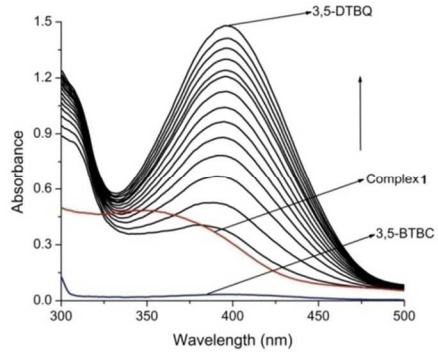

Fig. 9 Increase of the quinone band at around 400 nm after the addition of 100 equiv of 3,5-DTBC to an acetonitrile solution of complex **1**. The spectra were recorded at 5 min intervals.

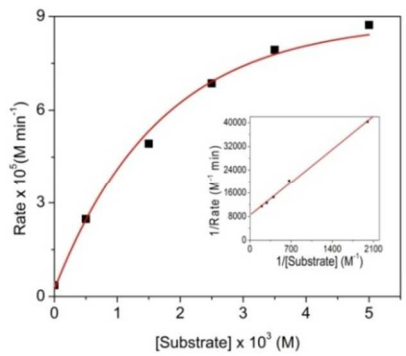

Fig. 10 Plot of the rate vs substrate concentration for complex **1**. Inset shows the corresponding Lineweaver−Burk plot.

To get a better understanding of the complex−substrate intermediate and a mechanistic inference of catecholase activity during the oxidation reaction, we have recorded ESI-MS spectra of **1**–**3**, and a 1:10 mixture of the complexes to and 3,5- DTBC within 10 min of mixing in acetonitrile solvent (Fig. S12−S17, Supporting Information). The spectrum of complexes **1** and **2** shows similar pattern. Both complexes show the base peak at m/z = 362.0 (100%), (calcd 362.0441) which can be assigned to the mononuclear species $[CoLNa]^+$. In addition, peaks due to the dinuclear $[Co_2L_2(CH_3CN)Na]^+$ and trinuclear $[Co_3L_2(N_3)_3]^+$ species at m/z = 743.1 and 863.0 respectively are also observed for both complexes. On the other hand, complex **3** displays a base peak at m/z = 366.0 (calcd 366.0754), which can be assigned to corresponding mononuclear species $[CoL^RNa]^+$ similar to **1** and **2**. Besides, the peak at m/z = 936.1 corresponding to Na-containing molecular ion of trinuclear species $[Co_3(L^R)_2(N_3)_4Na]^+$ appears in this spectrum. After the addition of 3,5-DTBC to the solutions of complexes **1–3**, drastic changes are observed in all three spectra. In case of **1** and **2**, in addition to the quinone sodium aggregate $[3,5\text{-DTBQ-Na}]^+$ at 243.1 (calcd 243.1415), the base peak at m/z = 921.2 (calcd 921.2449) corresponding to $[Co_2L_2(3,5\text{-DTBC})Na]^+$, and other peaks at m/z = 582.2 (calcd 582.1983), 1141.4 (calcd 1141.3912) and 701.1 (calcd 701.0985) corresponding to $[CoL(3,5\text{-DTBC})Na]^+$, $[Co_2L_2(3,5\text{-DTBC})_2Na]^+$ and $[Co_2L_2Na]^+$ respectively are generated. On the other hand, the spectrum of **3** exhibits a base peak at m/z = 586.2

View Article Online
DOI: 10.1039/C4DT03446E

(calcd586.2218) corresponding to $[CoL^R(3,5\text{-DTBC})Na]^+$ species. The peaks at m/z = 243.1 and 929.3 can be assigned to quinone sodium aggregate $[3,5\text{-DTBQ-Na}]^+$ and $[Co_2L^R{}_2(3,5\text{-DTBC})Na]^+$ respectively. These results reveal the formation of the catalyst–substrate as intermediates which take part in substrate activation during the oxidation of 3,5-DTBC to 3,5-DTBQ.

The mechanistic studies with copper-based model complexes are well established and it appears that there are two possible mechanisms for the oxidation of 3,5-di-tert-butylcatechol to their respective quinone. One proceeds through the formation of a dicopper(II) catecholate intermediate where the dicopper(II) species stoichiometrically oxidizes the catecholic substrate to one molecule of quinone and itself reduces to a dicopper(I) species. Then, the dicopper(I) species reacts with an oxygen molecule to generate a peroxo dicopper(II) adduct, which then oxidizes a second molecule of the substrate to quinone; water is formed as a byproduct through this four electron reduction process.[55] The second mechanism involves in the formation of an organic radical intermediate such as copper(I) semiquinonate.[56] Its subsequent reaction with dioxygen may result in the two electron reduction of dioxygen, leading to the reoxidation of the copper(I) ion and release of the quinone molecule, with hydrogen peroxide as a byproduct.[57]

In contrast, up to now there has been only limited study of plausible mechanisms of catechol oxidation reaction catalyzed by nickel(II), manganese(II/III) and zinc(II) complexes. However, it has been shown that the participation of metal centre in the catechol to quinone oxidation process is essential. Thus, this oxidation reaction catalyzed by either Ni(II) or Mn(III) complexes proceeds through the formation of semiquinonate intermediate species similar to Cu(II) complexes. Recently, we have studied the reaction mechanism of this oxidation reaction catalyzed by Ni(II)-oxime complexes[24] and shown that the reaction proceeds through the formation of Ni(III) species unlike the dicopper complexes where the oxidation states of Cu(II) shuttle between +I and +II. Moreover, Das *et.al* proposed that conversion of 3,5-DTBC to 3,5-DTBQ can be promoted by redox-innocent Zn(II) ion *via* radical pathway.[25] In this case, coordinated ligand undergoes reduction with concomitant oxidation of the catechol to form semibenzoquinone.

In order to get a preliminary idea about the mechanism of the catalytic reaction for these mixed valence Co(II)–Co(III) complexes, we were interested to know whether any H_2O_2 was formed and, if so, to find its amount. The estimation of H_2O_2 clearly shows that, after approximately 1 h of oxidation 91%, 79% and 82% H_2O_2 are generated with respect to the formation of 3,5-DTBQ for **1**–**3** respectively. The results indicate that nearly equimolar amount of hydrogen peroxide is formed with respect to 3,5-DTBQ. Therefore, keeping analogy to the mechanism of the oxidation by using the dicopper system, one might assume that the reaction proceeds through the formation of Co(II)-semiquinonate radical intermediate.

The valence states of cobalt (Co(II), Co(III)) and its spin state (Co(II) can exist in low spin S=1/2; or high spin, S=3/2 states) in complexes can be easily distinguished by EPR spectroscopy. In case of Co(III) ($3d^6$), the $t_{2g}^6 e_g^0$ configuration is diamagnetic and do not give any epr signal. In low spin state configuration Co(II) ($3d^7$) ($t_{2g}^6 e_g^1$; S=1/2), complexes with distorted octahedral or square planar geometries (C_{4v} or D_{4h} symmetry) having unpaired electron density localized in d_z^2 orbital, the principal values of g tensor is given by following equation

$$g_{\parallel} \approx g_e \text{ and } g_{\perp} = g_e + (\lambda/\Delta)$$

where g_e = 2.0023, λ is the spin orbit parameter and Δ is the energy difference between the $d_{xy,\ yz}$ and d_z^2. In such cases, epr signal is observed at room temperature due to sufficiently longer spin lattice relaxation time and they exhibit small anisotropy in g tensor ($g_{\perp} \sim 2.2 > g_{\parallel} = 2.02\text{-}2.01$). EPR parameters for low spin reported Co complexes are given in Table 6.[58] In high spin state configuration ($t_{2g}^5 e_g^2$; S=3/2), Co(II) can give epr signals with large anisotropy in g tensor (g_1=5.0-6.8, g_2=3.0-4.0 and g_3=2.5-1.85) and at very low temperatures. This is mainly due to short spin lattice relaxation time arising due to large orbital contribution of the unpaired electrons towards the magnetic moment of the ground state of Co(II) ion in octahedral field. Therefore, in order to understand the redox participation of the metal centers and to detect the organic radical, if any, produced as intermediate species, we have recorded the X-band EPR spectra of these three trinuclear Co(III)–Co(II)–Co(III) complexes, as well as the reaction mixtures in acetonitrile solutions at different temperatures and time intervals. The observed features of EPR spectra of all complexes in 10^{-3} M acetonitrile solutions at room temperature were similar. The spectra consisted of an isotropic signal at g *ca* 2.0045 having hyperfine structure comprised of eight lines of almost of equal intensities (A_{iso}= 10.57 G). This is shown in Fig. 11(a) (top). The hyperfine structure is due to interaction of unpaired electron with Co nuclei having nuclear spin I=7/2 (^{59}Co, I=7/2, 100% natural abundance). The existence of EPR signal at room temperature suggested presence of Co^{2+} in low spin state. The EPR spectra of frozen complexes in acetonitrile recorded at 100 K, showed two sets of eight lines, characteristic of the ^{59}Cohyperfine interaction and corresponding to the parallel and perpendicular directions of the symmetry axis with respect to the external magnetic field. The spectra were nearly axially symmetric with $g_{\parallel}$ = 2.0018, $A_{\parallel}$ = 19.65, $g_{\perp}$ =2.0059, $A_{\perp}$=7.0 G. The expected ground state for the Co^{2+}complexes can be expressed as $(d_{xz,yz})^4\ (d_{xy})^2(d_z^2)^1$. The observed epr parameters were consistent with the unpaired electron residing in the d_z^2 orbital. The typical EPR spectrum of complex **1** in acetonitrile is shown in fig. 11(a) (bottom).

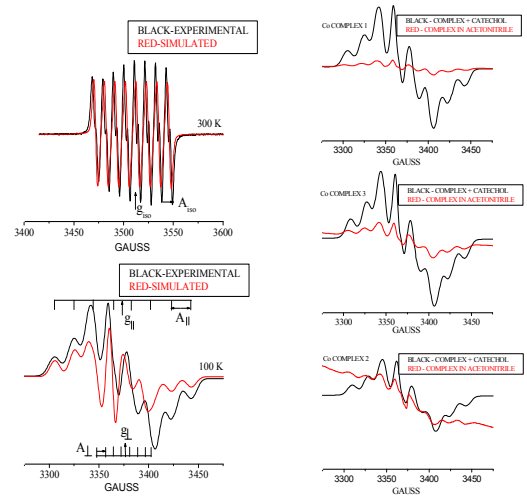

(a) (b)

Fig. 11 (a) The typical EPR spectrum of complex **1** in acetonitrile solution. The spectra in top and bottom were recorded at room temperature and 100K respectively. (b) The EPR spectra of different complexes with 3,5-DTBC in acetonitrile solutions recorded at room temperature.

View Article Online
DOI: 10.1039/C4DT03446E

The EPR spectra of 10^{-3} (M) each complexes with a 10^{-1} (M) 3,5-DTBC in acetonitrile solutions recorded at room temperature were similar to that of the complexes in 10^{-3} M acetonitrile without addition of 3,5-DTBC (no change in g and A value for Co^{2+}). However, initially there was a drastic increase in the intensity of the EPR signal upon addition of solution of 3,5-DTBC in acetonitrile which gradually increased further (Fig. 12). The increase in the integrated intensity followed the trend complex **1**> complex **3**> complex **2** (Fig. 12). The catecholase-like activity also followed similar trend complex **1**> complex **3**> complex **2** which is in accordance with the data obtained from optical absorption studies. This confirmed that reduction of some Co^{3+} sites to Co^{2+}occurred in all cases. However, we did not observe any signal corresponding to the formation of the semiquinonate radical intermediate presumably due to its transient nature.

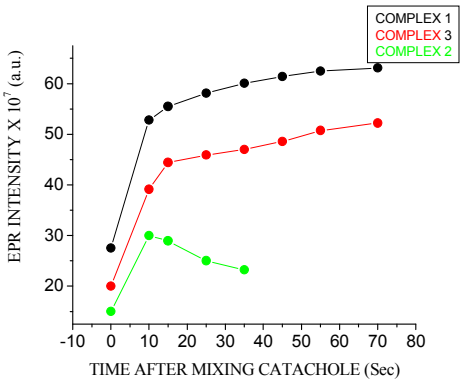

Fig. 12 The plots of EPR intensity *vs* the time after mixing the 3,5-DTBC to the different complexes (**1**–**3**).

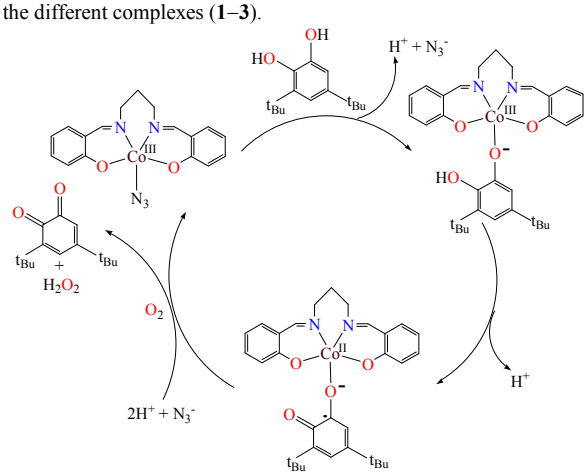

Scheme 3 Proposed mechanism for the catalytic cycle of the oxidation of 3,5-di-tert-butylcatechol by complex **1**. Complexes **2** and **3** show similar mechanism.

We therefore assume that the present compounds **1**–**3** catalyzes the oxidation of 3,5-DTBC to 3,5-DTBQ through the reduction of Co(III) to Co(II) where an organic radical intermediate such as Co(II)-semiquinonate species may be formed. The catalytic cycle is completed by the reaction of Co(II) species with dioxygen, leading to the reoxidation of the Co(II) to Co(III) ion and the reduction of dioxygen. Consequently, the quinone molecule as product and hydrogen peroxide as a byproduct are released. The probable reaction mechanism has been shown in Scheme 3.

Conclusion

In the present report, we have shown for the first time that the trinuclear mixed valence Co(II/III) complexes with a salen type Schiff base ligand can be isolated both in *cis* and *trans* configurations depending upon the solvent used for synthesis. The reduction of the Schiff base results in the formation of an unprecedented cyclic trinuclear mixed valence Co(II/III) complex in which a $\mu_{1,3}$–N_3 coordinated azido ligand participates in pnicogen bonding interactions as acceptor. From the DFT calculations, we have demonstrated that the *cis* isomers are energetically more stable and the *trans* isomer (observed experimentally in **2**) is stabilized by a hydrogen bonding network involving a water dimer that cannot be formed in compound **1**, which compensates the energy of less favored *trans* coordination. By means of MEP surfaces and CSD search we have demonstrated hitherto unnoticed counterintuitive electron acceptor ability of the $\mu_{1,3}$–N_3 coordinated azide ligand. All three complexes exhibit good catecholase-like activity in the aerial oxidation of 3,5-di-tert-butylcatechol to the corresponding o-quinone. Mechanistic investigations of the catalytic behaviors of these mixed valence Co(II/III) complexes by electrospray ionization mass (ESI-MS positive), estimation of hydrogen peroxide formation and EPR spectroscopy indicate that, similarly to the copper(II) analogues, the participation of metal centers through a cobalt(III)/cobalt(II) redox process is responsible for the oxidation of catecholic substrate to quinine.

Acknowledgement

A.H. and L.K.D. are thankful to CSIR, India, for awarding Junior Research Fellowship and Senior Research Fellowship respectively [Sanction No. 09/028 (0889)/2012-EMR-I dated 13/12/2012 for A.H. and 09/028 (0805)/2010-EMR-I for L.K.D.]. We thank Prof. M. G. B. Drew, School of Chemistry, The University of Reading, U.K. for the refinement of the structure of complexes **1-3**. Crystallography was performed at the DST-FIST, India, funded Single Crystal Diffractometer Facility at the Department of Chemistry, University of Calcutta. The authors also thank the Department of Science and Technology (DST), New Delhi, India, for financial support (SR/S1/IC/0034/2012). AB and AF thank the DGICYT of Spain (projects CTQ2011-27512/BQU and CONSOLIDER INGENIO 2010 CSD2010-00065, FEDER funds) and the Direcció General de RecercaInnovacióDel Govern Balear (project 23/2011, FEDER funds) for financial support.

Notes

[a]*Department of Chemistry, University College of Science, University of Calcutta, 92, A.P.C. Road, Kolkata-700 009, India. E-mail: ghosh_59@yahoo.com*
[b]*Radiochemistry Division, Bhabha Atomic Research Centre, Trombay, Mumbai 400085, India*
[c]*Department of Chemistry, Universitat de les IllesBalears, Crta de Valldemossa km 7.5, 07122 Palma de Mallorca, Baleares, Spain. E-mail: toni.frontera@uib.es*
*Electronic supplementary information (ESI) available: The electronic supplementary information file contains Fig. S1–S17.CCDC 1033263-1033265 for **1**–**3** respectively.*

References

1 (*a*) V. I. Maleev, M. North, V. A. Larionov, I. V. Fedyanin, T. F. Savelyeva, M. A. Moscalenko, A. F. Smolyakov and Y. N. Belokon, *Synth.Catal.*, 2014, **356**, 1803–1810; (*b*) S. Shit, D. Saha, D. Saha, T. N. G. Row and C. Rizzoli, *Inorg. Chim. Acta*, 2014, **415**, 103–110; (*c*) Y. N. Belokon, V. I. Maleev, M. North, V. A. Larionov, T. F. Savel'Yeva, A. Nijland and Y. V. Nelyubina, *ACS Catalysis*, 2013, **3**, 1951–1955; (*d*) V. I. Maleev,

View Article Online
DOI: 10.1039/C4DT03446E

M. North, V. A. Larionov, I. V. Fedyanin, T. F. Savel'Yeva, M. A. Moscalenko, A. F. Smolyakov and Y. N. Belokon, *AdvancedSynthesis and Catalysis*, 2014, **356**, 1803–1810; (*e*) E. Vinck, E. Carter, D. M. Murphy and D. S. Van, *Inorg. Chem.*, 2012, **51**, 8014–8024; (*f*) T. Kurahashi and H. Fujii, *Inorg.Chem.*, 2013, **52**, 3908–3919; (*g*) M. Lashanizadegan and Z. Zareian, *Catal. Lett.*,2011, **141**, 1698–1702.

2 (*a*) M. Hoshino, R. Konishi, N. Tezuka, I. Ueno and H. Seki, *Journal of Physical Chemistry*, 1996, **100**, 13569–13574; (*b*) H. Kunkely and A. Vogle, *Journal of Photochemistry and Photobiology A: Chemistry*, 2001, **138**, 51–54; (*c*) Y. Ohashi, *Bulletin of the Chemical Society of Japan*,1997, **70**, 1319–1324.

3 (*a*) M. Volpe, H. Hartnett, J. W. Leeland, K. Wills, M. Ogunshun, B. J. Duncombe, C. Wilson and J. B. Love, *Inorg. Chem.*, 2009, **48**, 5195–5207; (*b*) T. Honda, T. Kojima and S. Fukuzumi, *J. Am. Chem. Soc.*, 2012, **134**, 4196–4206; (*c*) A. Kamath, N. V. Kulkarni, P. P. Netalkar and V. K. Revankar, *SpectrochimicaActa - Part A: Molecular and Biomolecular Spectroscopy*, 2011, **79**, 1418–1424; (*d*) S. Durmus, A. Atahan and M. Zengin, *SpectrochimicaActa - Part A: Molecular and Biomolecular Spectroscopy*, 2011, **84**, 1–5.

4 (*a*) D. C. Ware, B. D. Palmer, W. R. Wilson and W. A. Denny, *J. Med. Chem.*,1993, **36**, 1839–1846; (*b*) P. K. Mascharak, *Coord. Chem. Rev.*, 2002, **225**, 201–214; (*c*) O. A. El-Gammal, E.-R. G. Abu and S. F. Ahmed, *SpectrochimicaActa Part A: Molecular and Biomolecular Spectroscopy*, 2015, **135**, 227–240; (*d*) M. Salehi, M. Amirnasr, S. Meghdadi, K. Mereiter, H. R. Bijanzadeh and A. Khaleghian, *Polyhedron*, 2014, **81**, 90–97; (*e*) F.-L. Mao and C.-H.Dai, *Synthesis and Reactivity in Inorganic, Metal-Organic, and Nano-Metal Chemistry*, 2014, **44**, 1059–1063; (*f*) K. Das, A. Datta, P.-H.Liu, J.-H.Huang, C.-L.Hsu, W.-T. Chang, B. Machura and C. Sinha, *Polyhedron*, 2014, **71**, 85–90.

5 (*a*) S. Chattopadhyay, M. G. B. Drew and A. Ghosh, *Eur. J. Inorg. Chem*., 2008, 1693–1701; (*b*) S. Banerjee, J.-T.Chen and C.-Z. Lu, *Polyhedron*, 2007, **26**, 686–694.

6 (*a*) G. E. Assey, R. J. Butcher and Y. Gultneh, *ActaCrystallogr.,Sect.E: Struct. Rep. Online*, 2011, **67**, m303–m304; (*b*) S. Chattopadhyay, G. Bocelli, A. Musatti and A. Ghosh, *Inorg. Chem. Comm.*, 2006, **9**, 1053–1057.

7 L. Mechi, P. Siega, R. Dreos, E. Zangrando and L. Randaccio, *Eur. J. Inorg. Chem.*, 2009, 2629–2638.

8 A. Ray, G. M. Rosair, R. Kadam and S. Mitra, *Polyhedron*, 2009, **28**, 796–806.

9 C. Fukuhara, E. Asato, T. Shimoji, K. Katsura, M. Mori, K. Matsumoto and S. Ooi, *J. Chem. Soc., Dalton Trans.*, 1987, 1305–1311.

10 X. He, C.-Z. Lu and C.-D. Wu, *J. Coord. Chem.*, 2006, **59**, 977–984.

11 (*a*) P. Seth, S. Ghosh, A. Figuerola and A. Ghosh, *Dalton Trans.*, 2014, **43**, 990–998; (*b*) C. Chen, D. Huang, X. Zhang, F. Chen, H. Zhu, Q. Liu, C. Zhang and L. Sun, *Inorg. Chem.*, 2003, **42**, 3540–3548.

12 (*a*) D.-H. Shi, Z.-L.You, C. Xu, Q. Zhang and H.-L. Zhu, *Inorg. Chem. Comm.*, 2007, **10**, 404–406; (*b*) A. Gerli, K. S. Hagen and L. G. Marzilli, *Inorg. Chem.*,1991**, 30,** 4613–4616.

13 (*a*) P. Mukherjee, M. G. B. Drew, C. J. Gómez-García and A. Ghosh, *Inorg. Chem.*, 2009**, 48***,* 4817–4827; (*b*) R. Biswas, S. Mukherjee, P. Kar and A. Ghosh, *Inorg.Chem.*, 2012, **51**, 8150−8160.

14 (*a*) C. Biswas, M. G. B. Drew, E. Ruiz, M. Estrader, C. Diaz and A. Ghosh, *Dalton Trans*., 2010, **39**, 7474–7484; (*b*) B. Sarkar, M. G. B. Drew, M. Estrader, C. Diaz and A. Ghosh, *Polyhedron*, 2008, **27**, 2625–2633.

15 (*a*) L. K. Das, S.-W. Park, S. J. Cho and A. Ghosh, *Dalton Trans*., 2012, **41**, 11009–11017.

16 A. Biswas, M. G. B.Drew, C. J. Gómez-García and A. Ghosh, *Inorg. Chem*., 2010, **49**, 8155–8163.

17 A. Hazari, L. K. Das, A. Bauzá, A. Frontera and A. Ghosh, *Dalton Trans*., 2014, **43**, 8007–8015.

18 A. Rompel, H. Fischer, D. Meiwes, K. Büldt-Karentzopoulos, R. Dillinger, F. Tuczek, H. Witzel and B. Krebs, *J. Biol. Inorg. Chem.*,1999, **4**, 56–63.

19 I. A. Koval, P. Gamez, C. Belle, K. Selmeczi and J. Reedijk, *Chem. Soc. Rev*., 2006, **35**, 814−840.

20 (*a*) B. Sreenivasulu, M. Vetrichelvan, F. Zhao, S. Gao and J. J. Vittal, *Eur. J. Inorg. Chem*., 2005, 4635−4645; (*b*) N. A. Rey, A. Neves, A. J. Bortoluzzi, C. T. Pich and H. Terenzi, *Inorg. Chem.*, 2007, **46**, 348−350.

21 V. K. Bhardwaj, N. Aliaga-Alcalde, M. Corbella and G. Hundal, *Inorg. Chim.Acta*, 2010, **363**, 97−106.

22 P. Chakraborty, J. Adhikary, B. Ghosh, R. Sanyal, S. K. Chattopadhyay, A. Bauzá, A. Frontera, E. Zangrando and D. Das, *Inorg. Chem.*, 2014, **53**, 8257−8269.

23 P. Seth, L. K. Das, M. G. B. Drew and A. Ghosh, *Eur. J. Inorg. Chem*., 2012, 2232–2242.

24 L. K. Das, A. Biswas, J. S. Kinyon, N. S. Dalal, H. Zhou and A. Ghosh, *Inorg. Chem.*, 2014, **53**, 434−445.

25 R. Sanyal, S. K. Dash, S. Das, S. Chattopadhyay, S. Roy and D. Das, *J. Biol.Inorg.Chem.*, 2014, *DOI* 10.1007/s00775-014-1148-z.

26 P. Wang, G. P. A. Yap and C. G. Riordan, *Chem. Commun*., 2014, **50**, 5871−5873.

27 (*a*) M. R. Sundberg, R. Uggla, C. Viñas, F. Teixidor, S. Paavola and R. Kivekäs, *Inorg. Chem. Commun.*, 2007, **10**, 713–716; (*b*) S. Scheiner, *Acc. Chem. Res*., 2013, **46**, 280–288; (*c*) A. Bauzá, R. Ramis and A. Frontera, *J. Phys. Chem. A*, 2014, **118**, 2827–2834. (*d*) A. Bauzá, T. J. Mooibroek and A. Frontera, *ChemCommun*, 2014, DOI: 10.1039/C4CC09132A

28 L. K. Das, R. M. Kadam, A. Bauzá, A. Frontera and A. Ghosh, *Inorg. Chem.*, 2012, **51**, 12407−12418.

29 M. K. Taylor, J. Reglinski, L. E. A. Berlouis and A. R. Kennedy, *Inorg. Chim.Acta*, 2006, **359**, 2455−2464.

30 R. T. Weber, WIN-EPR SIMFONIA manual, 1995.

31 SAINT, version 6.02; SADABS, version 2.03, Bruker AXS, Inc., Madison, WI, 2002.

32 G. M. Sheldrick, *Program for Structure Solution*, 1997.

33 G. M. Sheldrick, *Program for Crystal Structure Refinement*, 1997.

34 A. L. Spek, *J. Appl. Crystallogr*., 2003, **36**, 7−13.

35 L. J. Farrugia, *J. Appl. Crystallogr*., 1999, **32**, 837−838.

36 L. J. Farrugia, *J. Appl. Crystallogr*., 1997, **30**, 565.

37 R. Ahlrichs, M. Bär, M. Hacer, H. Horn and C. Kömel, *Chem. Phys. Lett*., 1989, **162**, 165–169.

38 S. Grimme, J. Antony, S. Ehrlich and H. Krieg, *J.Chem. Phys*., 2010, **132**, 154104–19.

39 AIMAll (Version 13.05.06), Todd A. Keith, TK Gristmill Software, Overland Park KS, USA, 2013.

40. (*a*) M. Mitra, P. Manna, A. Bauzá, P. Ballester, S. Kumar Seth, S. R. Choudhury, A. Frontera and S. Mukhopadhyay, *J. Phys. Chem. B*, DOI: 10.1021/jp510075m; (*b*) S. Saha, A. Sasmal, C. R. Choudhury, G. Pilet, A. Bauzá, A. Frontera, S. Chakraborty and S. Mitra, *Inorg. Chim. Acta*, 2015, **425**, 211–220; (*c*) M. Mirzaei, H. Eshtiagh-Hosseini, A. Bauzá, S. Zarghami, P. Ballester, J. T. Maguee and A. Frontera, *CrystEngComm*, 2014, **16**, 6149−6158 (*d*) M. Mirzaei, H. Eshtiagh-Hosseini, Z. Karrabi, K. Molčanov, E. Eydizadeh, J. T.Mague, A. Bauzá and A. Frontera, *CrystEngComm*, 2014, **16**, 5352−5363

View Article Online
DOI: 10.1039/C4DT03446E

(*e*) A. Neves, L. M. Rossi, A. J. Bortoluzzi, B. Szpoganicz, C. Wiezbicki, E. Schwingel, W. Haase and S. Ostrovsky, *Inorg. Chem*., 2002, **41**, 1788−1794.

41 A. Biswas, L. K. Das, M. G. B. Drew, G. Aromí, P. Gamez and A. Ghosh, *Inorg. Chem.*, 2012, **51**, 7993−8001.

42 S. Biswas and A. Ghosh, *Journal of Molecular Structure*, 2012, **1019**, 32–36.

43 A. W. Addison, T. N. Rao, J. Reedijk, J. V. Rijn and G. C. Verschoor, *J. Chem. Soc., Dalton Trans*., 1984, 1349−1356.

44 S. Mukhopadhyay, D. Mandal, P. B. Chatterjee, C. Desplanches, J.-P. Sutter, R. J. Butcher and M. Chaudhury, *Inorg. Chem.*, 2004, **43**, 8501–8509.

45 A. Nangia, K. Biradha and G. R. Desiraju, *J. Chem. Soc., Perkin Trans.*,1996, **2**, 943−953.

46 J. M. Dominguez-Vera, J. Suarez-Varela, I. B. Maimoun and E. Colacio, *Eur. J. Inorg. Chem*., 2005, 1907−1912.

47 S. Demeshko, G. Leibeling, S. Dechert, S. Fuchs, T. Pruschke and F. Meyer, *ChemPhysChem*, 2007, **8**, 405−417.

48 G. A. McLachlan, G. D. Fallon, R. L. Martin, B. Moubaraki, K. S. Murray and L. Spiccia, *Inorg. Chem.*, 1994, **33**, 4663−4668.

49 M. Monfort, I. Resino, M. S. E. Fallah, J. Ribas, X. Solans, M. Font-Bardia and H. Stoeckli-Evans, *Chem. Eur. J*., 2001, **7**, 280−287.

50 (*a*) G. Sánchez-Sanz, C. Trujillo, M. Solimannejad, I. Alkorta and J. Elguero, *Phys. Chem. Chem. Phys.*, 2013, **15**, 14310–14318; (*b*) J. E. del Bene, I. Alkorta and J. Elguero, *J. Phys. Chem. A*, 2013, **117**, 6893–6903.

51 J. Mukherjee and R. Mukherjee, *Inorg. Chim.Acta*, 2002, **337**, 429−438.

52 F. Zippel, F. Ahlers, R. Werner, W. Haase, H.-F.Nolting and B. Krebs, *Inorg. Chem.*, 1996, **35**, 3409−3419.

53 A. Banerjee, A. Guha, J. Adhikary, A. Khan, K. Manna, S. Dey, E. Zangrando and D. Das, *Polyhedron*, 2013, **60**, 102–109.

54 (*a*) S. Majumder, S. Mondal, P. Lemoine and S. Mohanta, *Dalton Trans*., 2013, **42**, 4561–4569; (*b*) R. Modak, Y. Sikdar, S. Mandal and S. Goswami, *Inorg. Chem. Comm*., 2013, **37**, 193–196.

55 E. Monzani, L. Quinti, A. Perotti, L. Casella, M. Gulotti, L. Randaccio, S. Geremia, G. Nardin, P. Faleschini and G. Tabbi, *Inorg. Chem.*, 1998, **37**, 553−562.

56 (*a*) M. R. Mendoza-Quijano, G. Ferrer-Sueta, M. Flores-Álamo, N. Aliaga-Alcalde, V. Gómez-Vidales, V. M. Ugalde-Saldívara and L. Gasque, *Dalton Trans*., 2012, **41**, 4985−4997; (*b*) J. Ackermann, F. Meyer, E. Kaifer and H. Pritzkow, *Chem. Eur. J*., 2002, **8**, 247−258; (*c*) M. Kodera, T. Kawata, K. Kano, Y. Tachi, S. Itoh and S. Kojo, *Bull. Chem. Soc. Jpn*., 2003, **76**, 1957−1964; (*d*) I. A. Koval, K. Selmeczi, C. Belle, C. Philouze, E. Saint-Aman, I. Gautier- Luneau, A. M. Schuitema, M. V. Vliet, P. Gamez, O. Roubeau, M. Luken, B. Krebs, M. Lutz, A. L. Spek, J.-L. Pierre and J. Reedijk, *Chem. Eur. J*., 2006, **12**, 6138−6150.

57 (*a*) R. A. Peralta, A. J. Bortoluzzi, B. Szpoganicz, T. A. S. Brandaoa, E. E. Castellano, M. B. de Oliveira, P. C. Severino, H. Terenzi and A. Neves, *J. Phys. Org. Chem*., 2010, **23**, 1000−1013; (*b*) J. Balla, T. Kiss and R. F. Jameson, *Inorg. Chem*., 1992, **31**, 58−62; (*c*) K. Selmeczi, M. Reglier, M. Giorgi and G. Speier, *Coord. Chem. Rev*., 2003, **245**, 191−201.

58 (*a*) E. F. Vansant and J. H. Lunsford, *Chem. Comm*., 1972, 830−832; (*b*)R. F. Howe and J. H. Lunsford, *J. Am. Chem. Soc*., 1975, **97**, 5156–5159; (*c*) S. Fljlwara, T. Watanabe and H. Tadano, *J. Coord. Chem*., 1971, **1**, 195−206; (*d*) M. Baumgarten, C. J. Winscom and W. Lubitz, *Applied Magnetic Resonance*, 2001, **20**, 35−70; (*e*) Y. Nishida, A. Sumita and S. Kida, *Bull. Chem. Soc. Japan*, 1977, **50**, 759−760; (*f*) B. K. Santra and G. K. Lahiri, *J. Chem. Soc., Dalton Trans*., 1998, 139–145.

View Article Online
DOI: 10.1039/C4DT03446E

Tables (1-6)

Unprecedented structural variations in trinuclear mixed valence Co(II/III) complexes derived from a Schiff base and its reduced form: Theoretical studies, pnicogen bonding interactions and catecholase-like activities

Alokesh Hazari, Lakshmi Kanta Das, Ramakant M. Kadam, Antonio Bauzá, Antonio Frontera* and Ashutosh Ghosh*

Table 1 Bond distances (Å) and angles (°) for complexes **1**

	1A	**1B**		**1A**	**1B**
Co(2)–O(10)	1.908(1)	1.899(1)	O(10)–Co(2)– N(7)	89.2(4)	89.0(5)
Co(2)–O(30)	1.934(1)	1.928(1)	O(10)–Co(2)– N(1)	87.7(4)	87.5(4)
Co(2)–N(18)	1.928(1)	1.925(1)	O(30)–Co(2)– N(1)	81.0(4)	80.2(4)
Co(2)–N(22)	1.940(1)	1.933(1)	O(30)–Co(2)– N(7)	90.8(4)	91.2(4)
Co(2)–N(1)	1.991(1)	1.984(1)	N(22)–Co(2)– O(10)	174.0(4)	174.8(4)
Co(2)–N(7)	1.941(1)	1.937(1)	N(18)–Co(2)– O(30)	176.7(4)	175.7(5)
Co(3)–O(31)	1.885(1)	1.901(1)	N(7)–Co(2)– N(1)	171.3(5)	170.9(5)
Co(3)–O(51)	1.908(1)	1.916(1)	O(31)–Co(3)– O(51)	87.1(4)	86.8(4)
Co(3)–N(39)	1.916(1)	1.904(1)	N(39)–Co(3)– N(43)	94.7(4)	95.0(5)
Co(3)–N(43)	1.923(1)	1.945(1)	O(51)–Co(3)– N(43)	87.9(4)	88.1(4)
Co(2)–O(10)	1.908(1)	1.899(1)	O(31)–Co(3)– N(39)	90.7(4)	90.3(4)
Co(3)–N(4)	1.950(1)	1.944(1)	N(4)–Co(3)– N(43)	88.8(5)	89.9(5)
Co(3)–N(10)	1.987(1)	1.994(1)	N(39)–Co(3)– N(4)	91.8(5)	93.1(4)
Co(1)–O(30)	2.115(1)	2.112(1)	O(31)–Co(3)–N(4)	87.8(5)	87.6(5)
Co(1)–O(51)	2.115(1)	2.103(1)	O(51)–Co(3)–N(4)	91.7(4)	90.7(4)
Co(1)–N(10)	2.125(1)	2.119(1)	O(31)–Co(3)–N(43)	173.8(4)	174.3(4)
Co(1)–N(1)	2.109(1)	2.095(1)	O(51)–Co(3)–N(39)	175.7(4)	175.1(4)
Co(1)–O(1)	2.091(1)	2.075(1)	N(4)–Co(3)– N(10)	172.4(5)	171.1(4)
Co(1)–O(2)	2.090(1)	2.093(1)	O(51)–Co(1)–N(10)	73.4(4)	73.9(3)
O(10)–Co(2)– O(30)	87.1(4)	86.9(4)	O(30)–Co(1)–N(10)	92.5(4)	92.8(4)
N(18)–Co(2)– N(22)	95.3(5)	95.1(4)	O(30)–Co(1)–N(1)	74.2(4)	73.6(4)
O(30)–Co(2)– N(22)	87.1(4)	88.1(4)	O(30)–Co(1)–O(1)	81.8(4)	82.2(4)
O(10)–Co(2)– N(18)	90.6(4)	90.0(4)	N(1)–Co(1)–O(1)	90.7(5)	91.1(4)
N(22)–Co(2)– N(1)	93.0(4)	93.1(4)	O(30)–Co(1)–O(51)	111.8(4)	111.6(4)
N(22)–Co(2)– N(7)	89.2(5)	89.7(5)	N(10)–Co(1)–N(1)	157.6(4)	157.2(4)
N(18)–Co(2)– N(1)	96.6(4)	96.8(4)	O(30)–Co(1)–O(2)	168.7(4)	168.4(4)
N(18)–Co(2)– N(7)	91.5(4)	91.6(5)	O(1)–Co(1)–O(2)	87.3(4)	86.6(4)

View Article Online
DOI: 10.1039/C4DT03446E

Table 2 Bond distances (Å) and angles (°) for complexes **2**

Co(2)–O(10)	1.905(2)	O(30)–Co(2)– N(22)	88.9(6)	N(22)–Co(2)– O(10)	173.0(5)
Co(2)–O(30)	1.915(2)	O(10)–Co(2)– N(18)	90.4(6)	N(18)–Co(2)– O(30)	174.3(6)
Co(2)–N(18)	1.935(2)	N(22)–Co(2)– N(1)	90.7(6)	N(7)–Co(2)– N(1)	177.4(6)
Co(2)–N(22)	1.945(2)	N(22)–Co(2)– N(7)	87.8(7)	O(30)–Co(1)–N(1)	104.3(5)
Co(2)–N(1)	2.000(1)	N(18)–Co(2)– N(1)	93.9(6)	O(30)–Co(1)–O(1)	93.9(5)
Co(2)–N(7)	1.943(2)	N(18)–Co(2)– N(7)	88.4(6)	N(1)–Co(1)–O(1)	87.9(5)
Co(1)–O(30)	2.061(2)	O(10)–Co(2)– N(7)	93.0(6)	O(30)–Co(1)–O(30)[a]	180.0
Co(1)–N(1)	2.203(2)	N(18)–Co(2)– N(22)	96.5(6)	N(1)–Co(1)–N(1)[a]	180.0
Co(1)–O(1)	2.064(2)	O(10)–Co(2)– N(1)	88.2(6)	O(1)–Co(1)–O(1)[a]	180.0
O(10)–Co(2)–O(30)	84.2(5)	O(30)–Co(2)– N(1)	83.9(5)		
N(18)–Co(2)– N(22)	96.5(6)	O(30)–Co(2)– N(7)	93.9(6)		

Symmetry element [a] = 2-x,-y,-z for **2.**

Table 3 Bond distances (Å) and angles (°) for complexes **3**

Co(2)–O(10)	1.925(5)	O(30)–Co(2)– N(22)	92.8(2)	N(39)–Co(3)– N(3)	90.4(2)
Co(2)–O(30)	1.928(5)	O(10)–Co(2)– N(18)	92.4(2)	N(39)–Co(3)– N(4)	87.4(2)
Co(2)–N(18)	1.992(6)	N(22)–Co(2)– N(1)	86.9(3)	O(31)–Co(3)– N(3)	90.3(2)
Co(2)–N(22)	1.979(6)	N(22)–Co(2)– N(7)	89.0(3)	O(31)–Co(3)–N(4)	94.2(2)
Co(2)–N(1)	1.987(6)	N(18)–Co(2)– N(1)	90.6(2)	O(51)–Co(3)–N(3)	90.7(2)
Co(2)–N(7)	1.943(6)	N(18)–Co(2)– N(7)	87.1(2)	O(51)–Co(3)–N(4)	92.1(2)
Co(3)–O(31)	1.922(5)	O(10)–Co(2)– N(7)	93.8(2)	O(31)–Co(3)–N(43)	171.2(2)
Co(3)–O(51)	1.922(5)	O(10)–Co(2)– N(1)	90.7(2)	O(51)–Co(3)–N(39)	170.7(2)
Co(3)–N(39)	1.991(6)	O(30)–Co(2)– N(1)	90.5(2)	N(3)–Co(3)–N(4)	175.1(2)
Co(3)–N(43)	1.973(6)	O(30)–Co(2)– N(7)	92.5(2)	O(31)–Co(1)–O(51)	71.7(2)
Co(3)–N(3)	1.980(6)	N(22)–Co(2)– O(10)	170.9(2)	O(30)–Co(1)–O(10)	72.0(2)
Co(3)–N(4)	1.941(6)	N(18)–Co(2)– O(30)	170.8(2)	O(51)–Co(1)–N(10)	105.7(3)
Co(1)–O(10)	2.000(5)	N(7)–Co(2)– N(1)	175.1(2)	O(31)–Co(1)–N(10)	120.8(3)
Co(1)–O(30)	2.140(5)	O(31)–Co(3)– O(51)	78.3(2)	O(10)–Co(1)–N(10)	121.0(3)
Co(1)–O(31)	1.997(5)	N(39)–Co(3)– N(43)	96.0(2)	O(30)–Co(1)–N(10)	105.9(3)
Co(1)–O(51)	2.140(5)	O(51)–Co(3)– N(43)	93.3(2)	O(30)–Co(1)–O(31)	91.7(2)
Co(1)–N(10)	1.977(7)	O(31)–Co(3)– N(39)	92.5(2)	O(10)–Co(1)–O(51)	91.9(2)
O(10)–Co(2)– O(30)	78.5(2)	N(3)–Co(3)– N(43)	87.2(2)	O(10)–Co(1)–O(31)	118.2(2)
N(18)–Co(2)– N(22)	96.4(3)	N(4)–Co(3)– N(43)	88.6(2)	O(30)–Co(1)–O(51)	148.4(2)

Table 4 Kinetic Parameters for the Oxidation of 3,5-DTBC Catalyzed by Complexes **1**, **2** and **3**

Complexes	V_{max} (M min^{-1})	Std. error	K_M (M)	Std. error	K_{cat} (h^{-1})
1	11.8 X 10^{-5}	6.79 X 10^{-6}	1.89 X 10^{-3}	5.89 X 10^{-5}	142
2	7.17 X 10^{-5}	0.60 X 10^{-6}	1.44 X 10^{-3}	0.81 X 10^{-5}	85
3	8.29 X 10^{-5}	3.87 X 10^{-6}	1.65 X 10^{-3}	4.78 X 10^{-5}	99

View Article Online
DOI: 10.1039/C4DT03446E

Table 5 k_{cat} values for the oxidation of 3,5-DTBC to 3,5- DTBQ catalyzed by complexes **1**–**3** and other reported cobalt complexes

Complexes	$K_{cat}(h^{-1})$ in CH_3CN	$K_{cat}(h^{-1})$ in CH_3OH	References
$[Co^{III}Co^{II}L^1(N_3)_3]\cdot 0.5CH_3CN\cdot 0.27H_2O$	114.24	Not done	54(a)
$[Co_{III}Co_{II}L^1(N_3)_3]\cdot CH_3CN$	482.16	45.38	54(a)
$[Co_2(L^2H)(H_2O)_2(CH_3CO_2)_2](CH_3CO_2)_2$	Not done	447	53
$[Co_2(L^3)(H_2O)_2(CH_3CO_2)_2](CH_3CO_2)$	Not done	45.9	53
$[Co_2(L^4)(H_2O)_2(CH_3CO_2)_2](CH_3CO_2)$	Not done	42.9	53
Complex **1**	142	Not done	Present work
Complex **2**	85	Not done	Present work
Complex **3**	99	Not done	Present work

Where, H_2L^1 = The [2 + 2] condensation product of 2,6-diformyl-4-methylphenol and 2,2-dimethyl-1,3-diaminopropane, H_2L^2 = 2,6-bis(N-ethylpiperazine -iminomethyl)-4-methyl-phenol, H_2L^3 = 2,6-bis(2-ethylpyridine-iminomethyl)-4-methyl-phenol and H_2L^4 = 2,6-bis(N-ethylpiperidine-iminomethyl)-4-methyl-phenol.

Table 6 EPR parameter of low spin cobalt complexes (S=1/2) in different geometries (distorted octahedral, square pyramid or trigonal bipyramid and square planar coordination). Hyperfine coupling constant is given in Gauss

Matrix	g_1	g_2	g_3	A_1	A_2	A_3	References
$[Co(CH_3NC)_6]^{2+}$	2.008	2.087	2.087	68	72	72	58(a)
$[Co(CH_3NC)_5]^{2+}$	2.003	2.163	2.163	89	32	32	58(a)
Co(NH,),O,-Y	2.002	2.010	2.084	12.5	12	17.8	58(b)
Co(CH,NH,),O,-Y	1.999	2.010	2.075	12	12	21	58(b)
$Co(NH_3)_5O_2$	1.995	1.995	2.981	12.2	12.2	17.2	58(c)
$[Co(N)_4]^{2+}$	2.024	2.479	2.479	108	78	78	58(d)
$Co(N_2S_2)^{2+}$	2.000	2.000	3.39	---	---	165	58(e)
$[CoN_6]^{2+}/[CoN_4P_2]^{2+}$	2.003	2.003	2.009	---	---	6.78	58(f)
Co^{2+} complexes **1**,**2** & **3**	2.0018	2.0059	2.0059	19.65	7.0	7.0	Present work

Estimated errors for g value, ±0.002; for hyperfine splitting, ±0.5 G, complexes were frozen in acetonitrile solution